Chapter 1
Motion in Vacuum

1.1 Crystal Manipulator with Six Degrees of Motional Freedom

This design [1] is shown in two parts to separate the azimuthal motion (Fig. 1.1) device from the tilt motion device (Fig. 1.2). A central rod extends from a typical *x*, *y*, *z*-plus rotary motion manipulator. The azimuthal and tilt motion (pushing and pulling) devices are connected to the same central rod and are free to slide up and down on this rod. The central rod is slotted to keep the crystal mount linking fittings from rotating with respect to the rod. The two push-and-pull actuators permit the central rod that passes through them to rotate in two ball-bearing (BB) mounts. Azimuthal crystal motion is transmitted by the push-and-pull actuator, which, through two coupled universal joints, turns the crystal mounting platform on its own ball bearing mount behind. Tilt motion is transmitted by the push-and-pull actuator, which tilts the crystal mounting platform about the axis of the hexagonal nut shown in the Tilt Motion diagram. The degrees of freedom for motion at various points are shown by double-headed arrows. This design does not result in a decoupling of tilt motion from other degrees of freedom, which is a disadvantage in some cases, but the design has been used for more than ten years with success. A more recent design uses a circular slot to guide a pin in the crystal tilt mechanism that eliminates the crystal translational motion associated with the tilt motion. It is of interest to note that in this design, ordinary unlubricated ball bearings are used in ultrahigh vacuum with success and without seizure or binding.

The crystal is mounted on electrical and thermal isolation standoffs on the crystal mounting platform and may be heated by electron bombardment or by ohmic heating. Various thermocouples may be connected to the crystal, and cooling to about 40 K is achieved using a copper braid connected between the crystal mounting assembly and a liquid He cryostat. Appropriate provisions are made to shield the mounting assembly from emitted radiation generated during crystal heating so that the desorption of impurities from the mounting is minimized.

J.T. Yates Jr., *Experimental Innovations in Surface Science*,
DOI 10.1007/978-3-319-17668-0_1

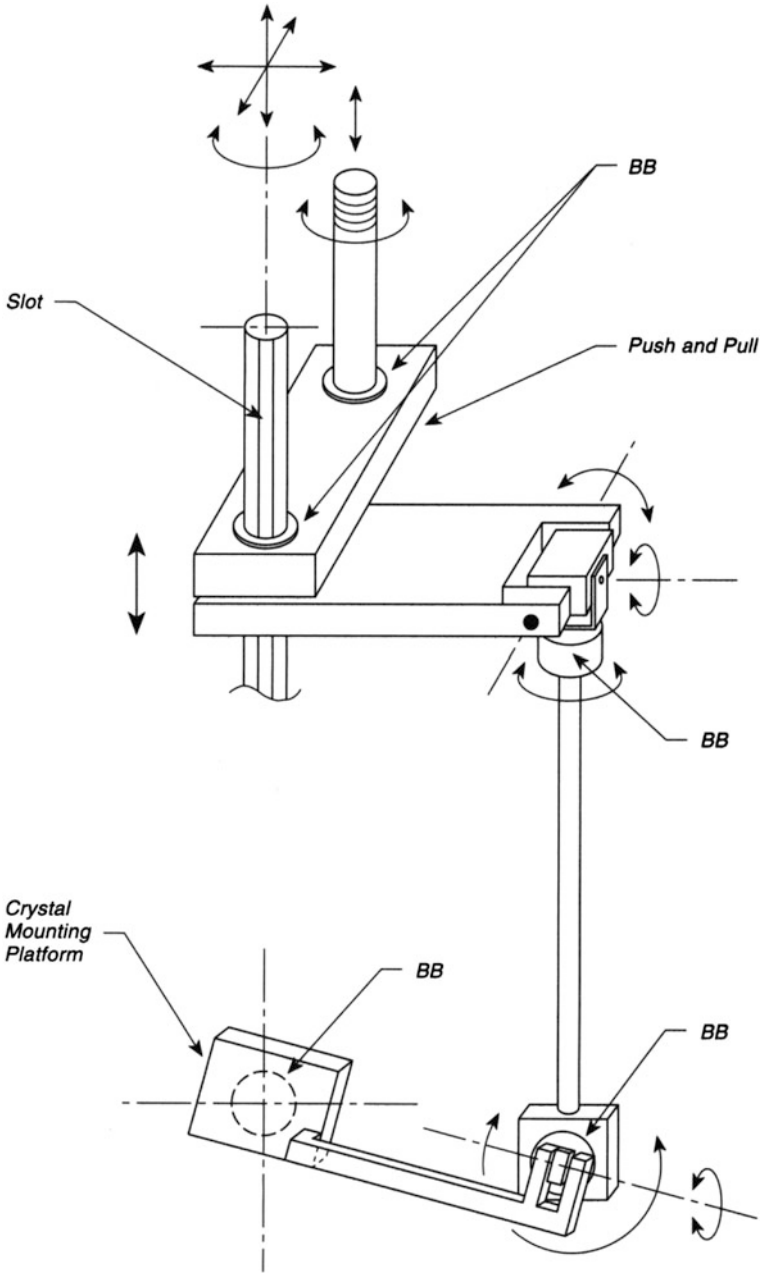

Fig. 1.1 Azimuthal motion

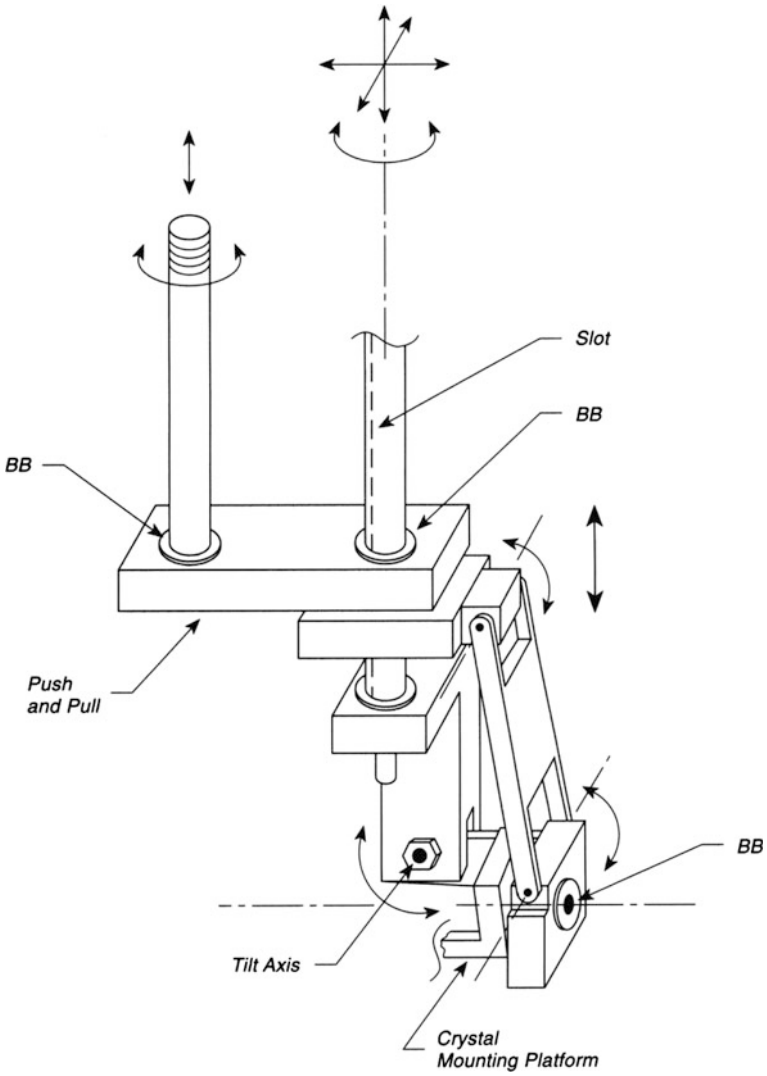

Fig. 1.2 Tilt motion

Because of the complexity of the design of a device of this sort, it is recommended that a working model first be constructed before final design parameters are set.

Many other designs allowing cooled crystals to be azimuthally rotated in ultrahigh vacuum have been published [2–12] and some are treated in this book.

1.2 Rotation in Ultrahigh Vacuum

The provision for rotation of samples in ultrahigh vacuum (UHV) is centrally import ant in most investigations, since the analytical facilities in most research chambers are located on different azimuths from the center line of the vacuum chamber. It is often desired to provide other motions, as well as heating and cooling of the crystal, but this section is concerned only with axial rotation. Historically, the problem was addressed in the first sixty inch cyclotron by Wilson [13], long before ultrahigh vacuum was achieved in metal systems. It is of interest to note that the differential pumping method employed by Wilson is still fundamentally important to UHV technology.

Figure 1.3 shows the Wilson seal as currently used in ultrahigh vacuum to rotate a long cylindrical cryostat on which the crystal is mounted using ceramic feed-throughs [14]. Two Viton gaskets, with a hole cut smaller than the rotary seal tube, are held in place in a brass housing that bolts onto a specially shaped lower Conflat flange having an upward-facing conical section to push the Viton gasket upward as shown. An assembly plate, below the upper Viton seal, also has an upward-directed conical support section. These two Viton seals make a strained contact with the polished-mirror-finished (600 grit) outer portion of the rotary seal, and provide the vacuum tight joint. To prevent significant leakage through the lower Viton seal gasket, the region between the two gaskets is differentially pumped with a rotary pump or a small ion pump. The cryostat tube, welded to a mini-Conflat flange is bolted to a mini-Conflat knife-edge sealing surface on top of the rotary seal. Two stabilizer bearings prevent wobbling of the central components; these may be made of phosphor bronze [14], Teflon, or they may even be ball bearings. Wires for heating the sample electrically, and thermocouple wires conveniently thread down the cryostat tube and exit from the bottom. As is obvious from the drawing, the bottom Con-flat flange must be bolted on from below, meaning that a flanged extension tube from the chamber flange must be employed under the device. A handle added to the flange of the rotary seal (not shown) is helpful in applying torque, and the upper section of the brass housing is divided into degrees of arc for accurate angular positioning, using the pointer. Bakeout temperatures of 150 °C are nondamaging to the Viton seals. For higher temperature bakeout, KALREZ per-fluoro elastomer might be used [15]. The gaskets can most conveniently be made by use of a homemade punching jig to accurately locate and cut the center hole to size as well as to place the six radial holes through which pass the bolts clamping the assembly plates down on the Viton. A pressure rise of about 1×10^{-10} Torr was observed on slow rotation.

The seal in Fig. 1.3 is designed for liquid nitrogen cooling, and in order to achieve long cryogenic storage time, a 1-L storage Dewar with a hole in its bottom was fabricated [16]. To make a liquid nitrogen seal each day with the cryostat tube, a platform support for the Dewar is covered with some cotton wool that is saturated with water; sufficient ice forms to make an excellent seal. Ice formation under the support platform by condensation from the atmosphere is a problem that can be

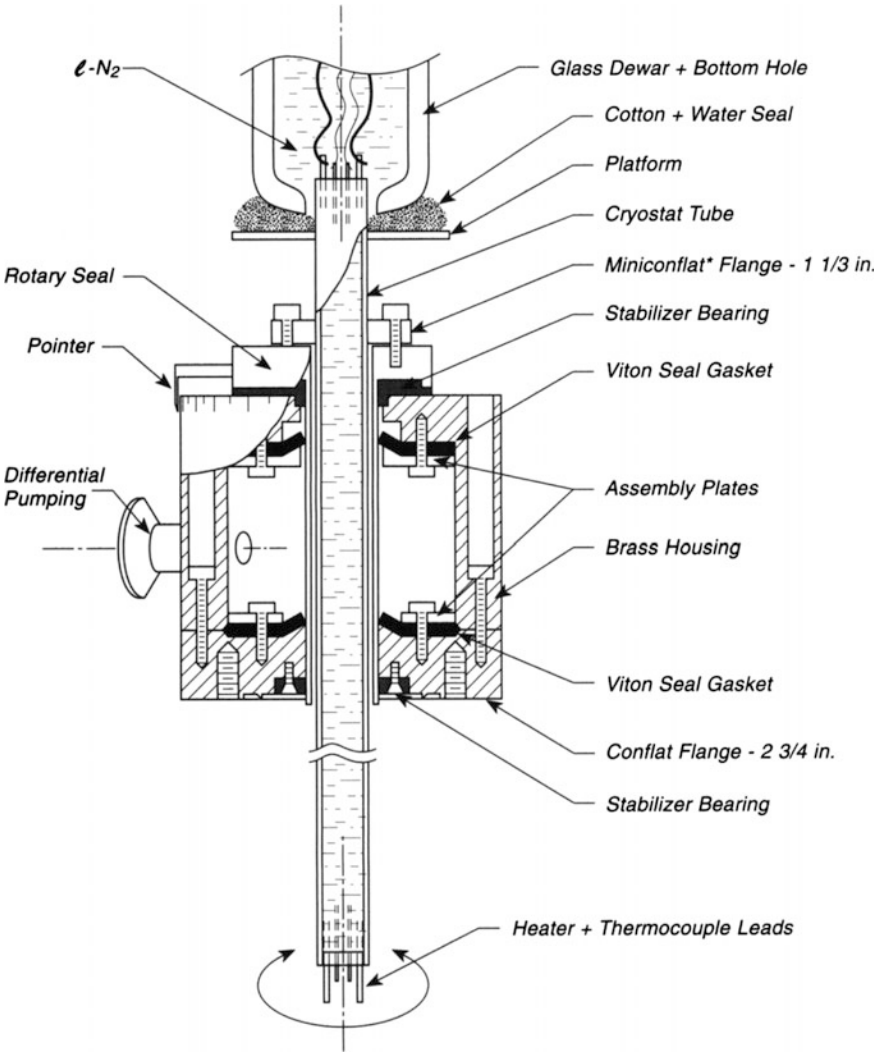

Fig. 1.3 Differentially pumped rotary seal—flat Viton gaskets

reduced by using a heater tape around the brass housing and possibly a fan to evaporate liquid water runoff. The apparatus can be inefficiently used with the gaseous discharge from a liquid He Dewar to achieve temperatures near 30 K, and the momentary transfer of liquid He brings the temperature to 15 K [14, 16]. Another rotary seal based on this principle has been reported [17].

Figure 1.4 shows a second design for a rotary seal in which O-rings are employed as the sealing elements, with one stage of differential pumping between the O-rings [18]. A polished rotary-seal tube rotates against the slightly compressed

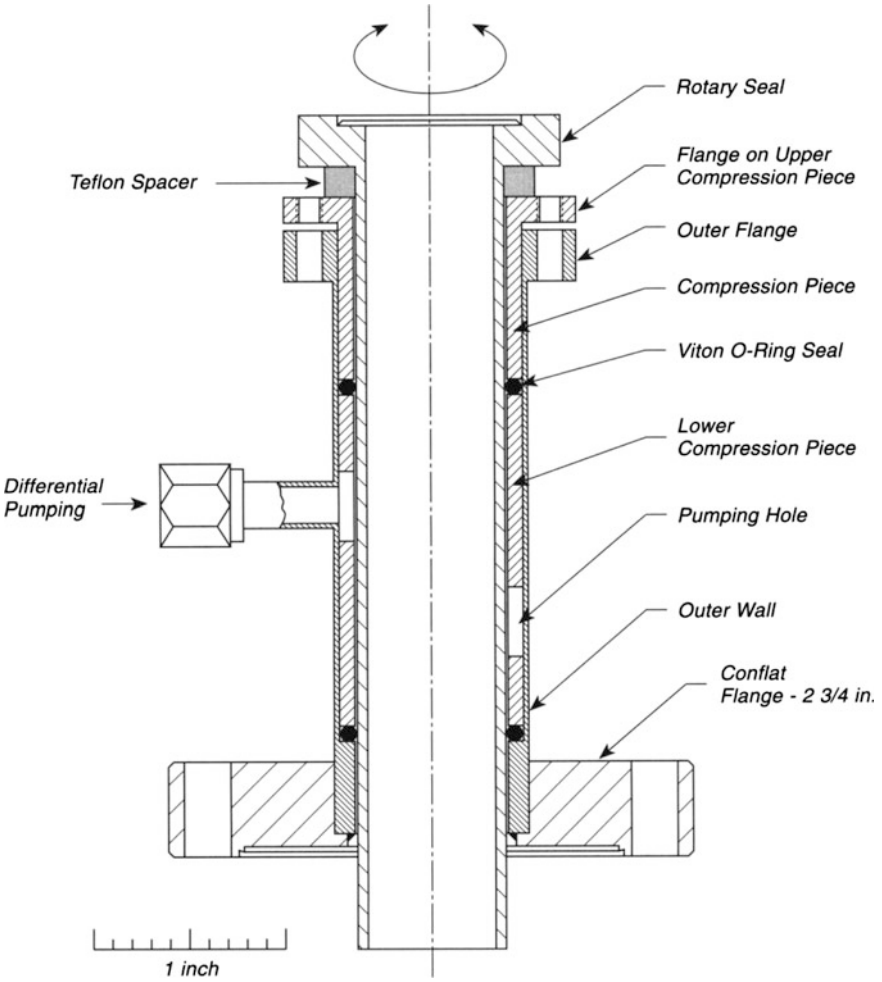

Fig. 1.4 Differentially pumped rotary seal—Viton O-ring

Viton O-rings, which are held in place by tightening the flange on the compression pieces, which are made of copper and which slide in between the outer wall and the rotary seal. These two compression pieces contain a number of holes to provide a pumping opportunity between the inside and outside of the cylindrical pieces. The O-rings are lubricated with a trace of graphite powder. A different lubricant reported to be satisfactory for Viton O-rings consists of a mixture of graphite powder and Santovac 5 diffusion pump oil (a polyfluo-roether) [19]. Differential pumping with a rotary pump or a small ion pump is used for the inner section holding the lower compression piece. A Teflon spacer at the top supplies a bearing surface for the rotary seal. Inside the rotary seal, a cryostat tube similar to that in Fig. 1.3 may be inserted. A pressure rise of about 3×10^{-11} Torr was observed on rotation [18].

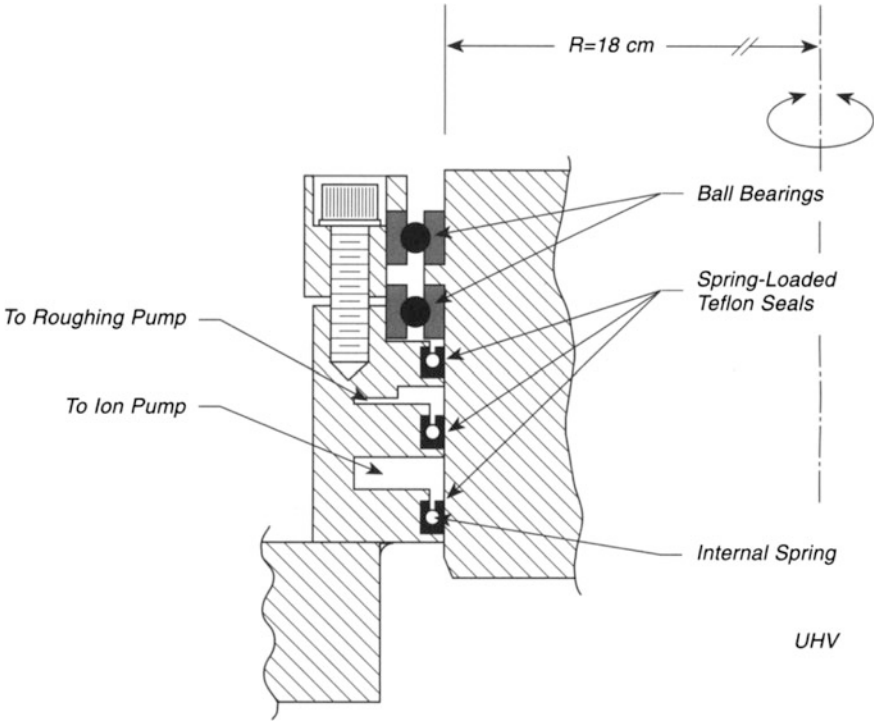

Fig. 1.5 Differentially pumped rotary seal—spring-loaded Teflon seals spring-loaded Teflon

Rotation using large differentially pumped seals is often employed to move heavy instruments inside the vacuum system, with a large-diameter rotating plate being moved through 360°. Auerbach [20] and his colleagues first reported the use of spring-loaded Teflon seals in this role in ultrahigh vacuum systems. Ordinary Teflon has a high thermal expansion coefficient, poor creep characteristics, and high permeability in static systems, so that differential pumping is required, along with a mechanical trick in which a spring is embedded inside the Teflon ring [21] to compensate for creep. These seals can also be obtained with Teflon filled with MoS2 lubricant particles for ultimate lubrication of an already lubricious material [20]. However, the filled polymer has a higher gas permeability than pure Teflon. In Fig. 1.5, a diagram of a double-stage differentially pumped Teflon seal is shown [20]. The large-diameter rotating plate is centered with two ball bearings, which have been split at the inner and outer races to prevent distortion and binding owing to differences in expansion coefficient between the bearings and the stainless steel. Beneath the ball bearings are three spring-loaded Teflon seals. The space between the upper two seals is pumped with a rotary pump, while a small ion pump [11 L/s]

pumps the space above the inner seal and the center seal. The system is baked to 200 °C, and the pressure rise upon rotation is less than 10^{-10} Torr and usually unobservable. The pressure at the small ion pump is in the 10^{-8} Torr range. The estimated gas leakage under static conditions is 10^{-13} Torr L/s [20]. Seals based on this principle are now commercially available. Others have reported the use of this type of seal for rotary manipulators [22–24].

Sometimes rapid rotation in ultrahigh vacuum is desired, where rather massive components must turn in bearings. Figure 1.6 shows a magnetically driven rotation

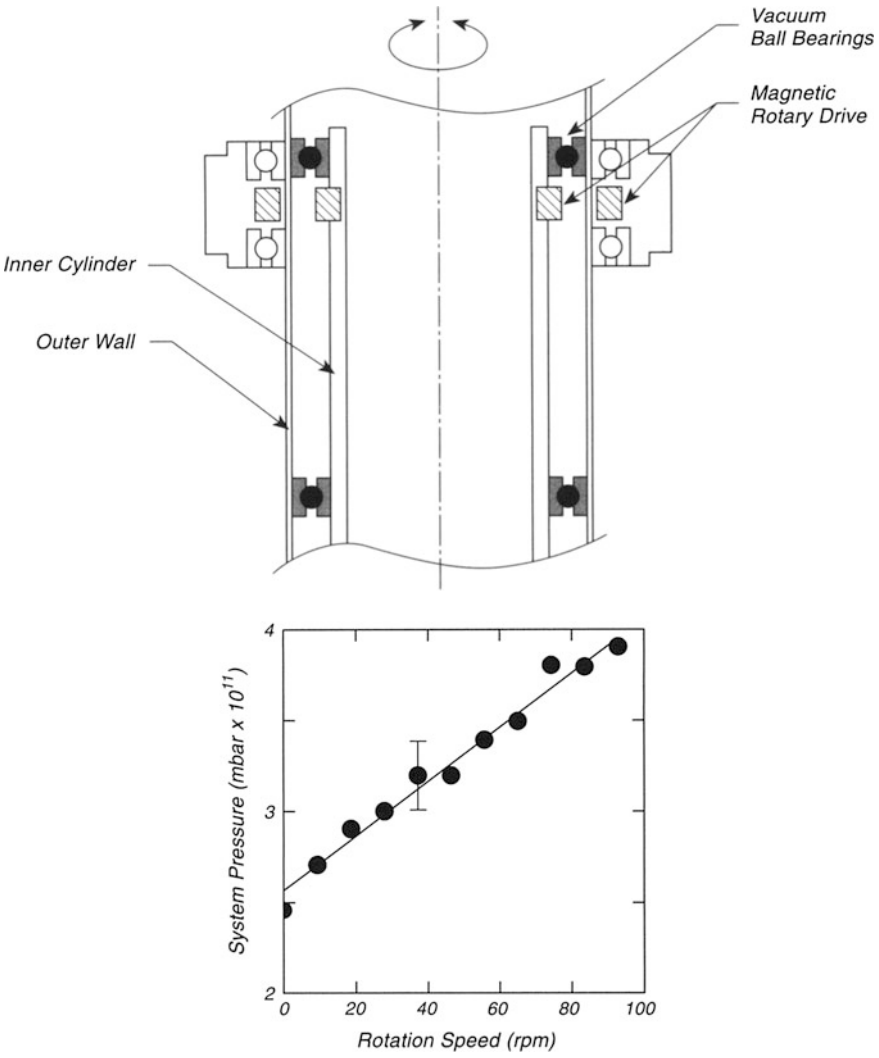

Fig. 1.6 Internal ball bearings

device that drives an inner cylinder suspended in vacuum. Two vacuum ball bearings are used at either end of the inner cylinder. These are ordinary ball bearings that are unlubricated, and they contain large cross section ball races. These bearings are routinely baked at 220 °C, and proved satisfactory for 18 months, having undergone 5×10^6 rotations without any degradation in performance. The evolution of gases is proportional to the rotation speed as shown in the lower part of Fig. 1.6, and the rise in total pressure is about 2×10^{-11} mbar at 100 rpm. Most of the gas evolution was due to H_2O and H_2 liberation [25].

Other designs for achieving independent rotational motions around two axes are described in the literature [26–28]. Reference [26] describes an electrical readout for the angular motions accurate to 0.5° and based on motion of a wire-wound potentiometer.

1.3 Crystal Positioning Using Capacitance

The ability to position a single crystal precisely can be useful in many measurement procedures in ultrahigh vacuum. This is a problem when the positioning must be done at accuracies beyond the capability of micrometer drives on manipulators. Factors such as thermal expansion effects, backlash in precision screw drives, and vibration interfere with accurate positioning methods.

The topic of capacitive positioning of a single crystal is treated in the context of locating the crystal accurately in front of a mass spectrometer that is housed in an apertured shield for accurate and reproducible temperature programmed desorption measurements [29]. This connects to the topic on p. 259.

Figure 1.7a shows a glass shield [29, 30] mounted over a quadrupole mass spectrometer ionization source. A Ta ring is rigidly supported near the aperture of the shield and acts as the capacitive pickup terminal. The capacitance is of the order of 0.1 pF for a 1-mm spacing between the Ta ring and the crystal. The capacitance measuring circuit, to be described below, can measure capacitance changes in the range of 0.1 %, meaning that the crystal can be positioned to 1 μm reproducibility, corresponding to an error in the measurement of the desorption rate from the crystal of only about 0.05 %. Small tilting of the crystal will reduce this reproducibility, and the demonstrated reproducibility of actual measurements was better than 1 % [30].

Figure 1.7b shows a slight variation on the design. Here, an Ag ring is employed as the capacitance pickup terminal, and it is fixed on the end of the glass shield as shown. The Ag plate, (12 mm OD; 6 mm ID, 1 mm thick) is held in place by use of 3 Ta wires that are spotwelded to the plate and wound around three glass eyelets on the shield. The Ag plate is connected through a Kapton-insulated and shielded lead to a BNC connector that exits the vacuum system. To avoid static charging, the glass shield is surrounded by a very thin grounded metal mesh [31]. An Aquadag [32] (colloidal graphite) coating can also be used for this purpose, or a metal shield like that shown on p. 260 may be used. The spacing employed between the crystal

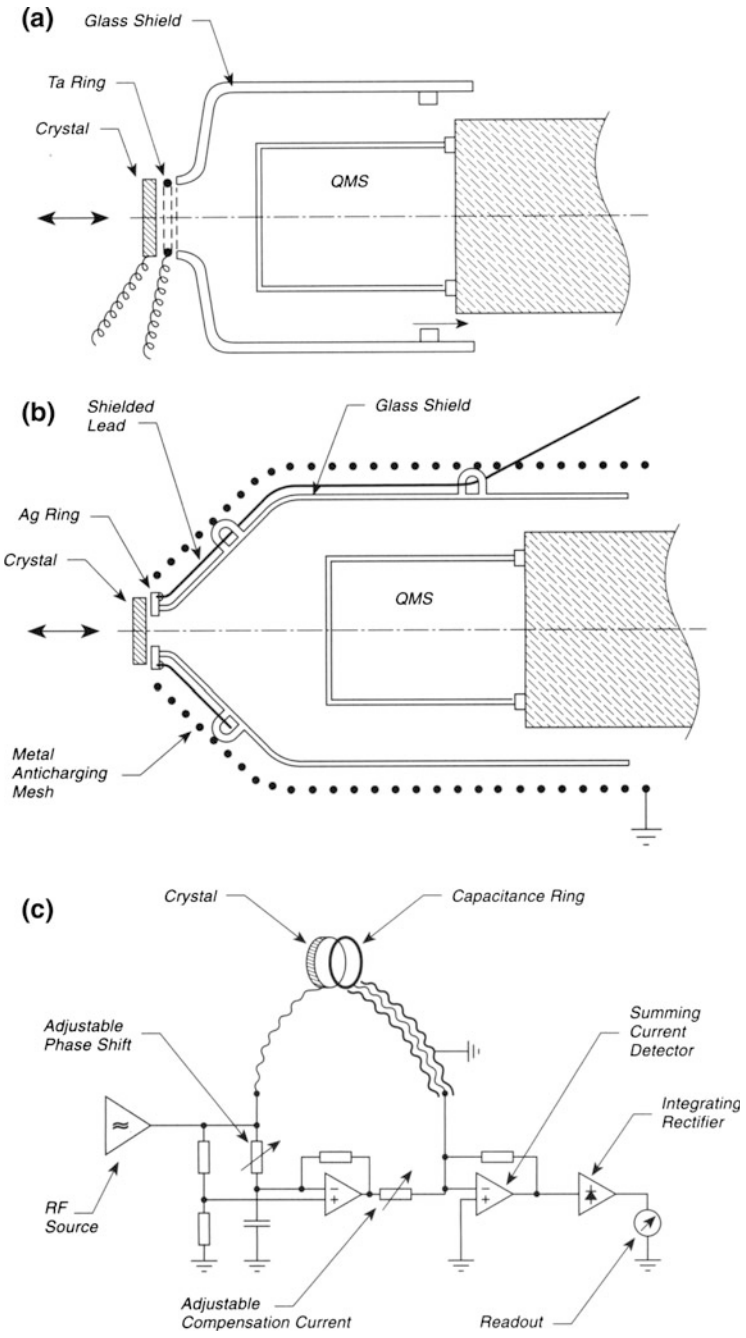

Fig. 1.7 Crystal positioning using capacitance. **a** Ring capacitance. **b** Affixed capacitance. **c** Capacitance measurement—block diagram

and the aperture is reported to be only 10 μm in this design, and this maybe reproduced to 1 μm [31].

The capacitance measuring circuit [30, 31] is shown in schematic block diagram form in Fig. 1.7c. It is a phase-shifted bridge circuit, working at 20 kHz [30]. A sinusoidal signal (20 Vpp) is applied to the crystal and the capacitive pickup is made to the ring aperture, since the crystal is often connected to unshielded leads and electronics outside of the vacuum system. The detection system is used as a simple lock-in amplifier.

1.4 UHV Rotary Manipulator with Arcsec Resolution

In some cases, the use of a commercial crystal manipulator is inappropriate because of the poor resolution and reproducibility inherent in these designs. For certain cases, such as in X-ray standing wave spectroscopy (XSW), a high-precision rotary stage is needed [33].

Figure 1.8a shows a side view of an ultrahigh vacuum system containing both a coarse and a fine adjustment for rotating a single crystal about the horizontal axis. The crystal holder is mounted on a platform such that its surface is in a plane that contains the axis of the shaft that holds the crystal holder. This shaft, made of precision-ground 304 stainless steel, rotates and translates inside of two linear/rotary ball bearings that are mounted on the top flange. With a conventional rotary feedthrough and rotary manipulator contacted to the shaft by a U-joint, coarse sample manipulation in 7 arcsec increments can be achieved with a stepping motor/speed reducer.

Figure 1.8b shows the principle of the high-precision rotary device, where the shaft may be engaged by a lever, and where precise variations in the position of the top of the shaft may be used to make azimuthal rotations to better than arcsec accuracy and precision.

Figure 1.8c shows the detailed structure of the high-precision rotary device coupled to the upper flange by a bellows. The rotary feedthrough drives an actuating lever that pushes a pushrod and the lower clutch body against two springs. When the force on the pushrod is released, the upper and lower clutch bodies grab the shaft. The rotation of the shaft about its axis is determined by the setting of the upper micrometer which is driven by a stepping motor. A weight is used to maintain tension and contact between the upper micrometer and the movable flange, and incremental motion of 0.88 arcsec is achieved with a lever arm of 292 mm length and a micrometer displacement of 1.25×10^{-3} mm [33].

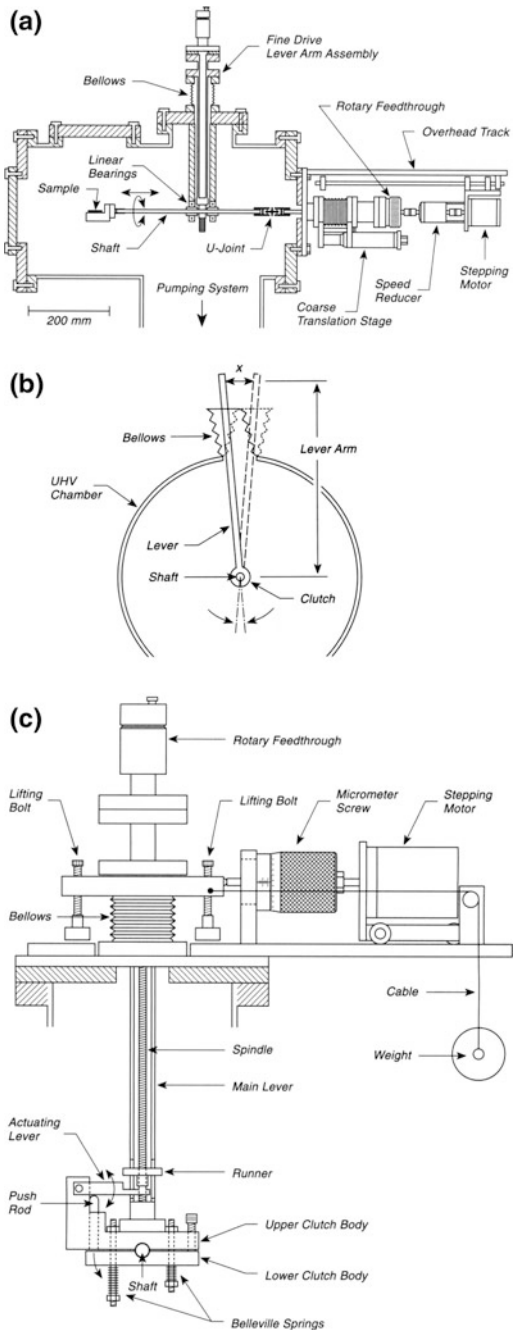

Fig. 1.8 Rotary motion—arcsec resolution. **a** Side view—coarse and fine adjustments. **b** Schematic—fine angular adjustment. **c** Detail—fine angular adjustment

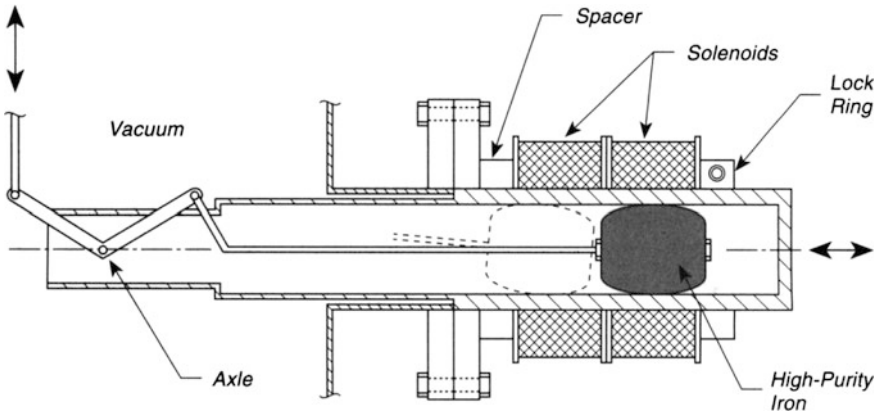

Fig. 1.9 Linear motion actuator

1.5 Solenoid Driven Linear Motion Device

A rapid linear motion inside an ultrahigh vacuum system may be achieved by using a solenoid-power-driven actuator like that shown in Fig. 1.9. All moving parts are inside the vacuum system, and the external solenoids do not require vacuum encapsulation. The actuator is a barrel-shaped plunger made of high-purity iron sized to make a loose fit inside the stainless steel tube. In this device a stroke of 3 cm was achieved. Each solenoid consists of 1400 turns of #24 magnet wire wound on an aluminum spool and giving a dc resistance of 14 Ω. Short electrical pulses are used on either solenoid to move the actuator in or out; the current is then turned off to prevent overheating or stray magnetic fields. In operation, the actuator will tilt as shown in the drawing when it moves inward. Measurements made on the actuator show that a torque of 500 g cm can be achieved at the internal pivot point. The closing time was measured to be 50 ms. The original paper [34] also provides a design for either an automatic or manual actuator circuit.

The solenoids are removed for system bakeout by releasing the lock ring on the back end. A similar magnetically driven shutter assembly using a Nd Fe-B magnetic encapsulated slug and an external ceramic-ring magnet has also been described [35].

1.6 An Inexpensive Linear Motion Device

A homemade linear motion device may be constructed quite easily from an inexpensive machinist's device as shown in Fig. 1.10. The vise is made of high-grade gray iron and the jaws as received from the manufacturer are precision ground for squareness and parallelism to ±0.0001 cm per cm. The hardened jaw pieces are

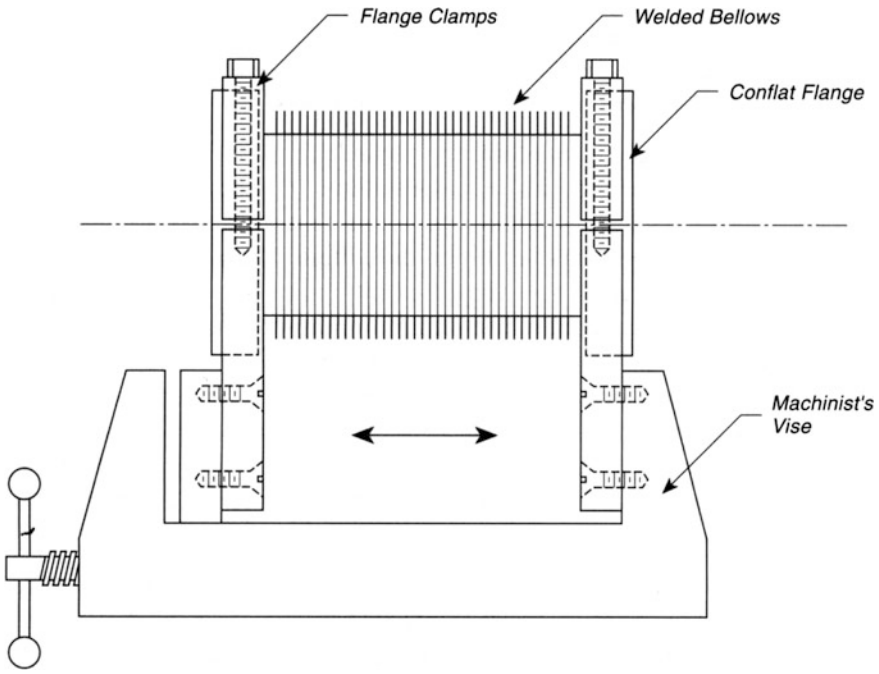

Fig. 1.10 Linear translation device

removed from the vise and replaced with aluminum clamps that have an inner lip machined in them to prevent the Conflat flanges from slipping through. These clamps are mounted on the vise and then tightened around the flanges holding the welded bellows. Machinist's vises giving up to 7.5 cm linear travel are available [36] at a cost of about $200–$300, and this device, while heavy, gives smooth and repeatable translation. The precise position can be determined using a vernier caliper between the clamps, or repeatable positions can be established by using simple spacer bars. The overall price is about a quarter that of a comparable commercial bellows manipulator [37].

1.7 Translating Auger Spectrometer

It is sometimes appropriate to move an Auger spectrometer or other large instrument over a large distance. This may be done in a conventional fashion by using a large-bellows translation device, which is both heavy and expensive. An alternate method for achieving the same result is to employ internal linear ball bearings and to translate with a small bellows-type linear translator. This requires that the electrical connections to the instrument be flexible over rather long extension distances.

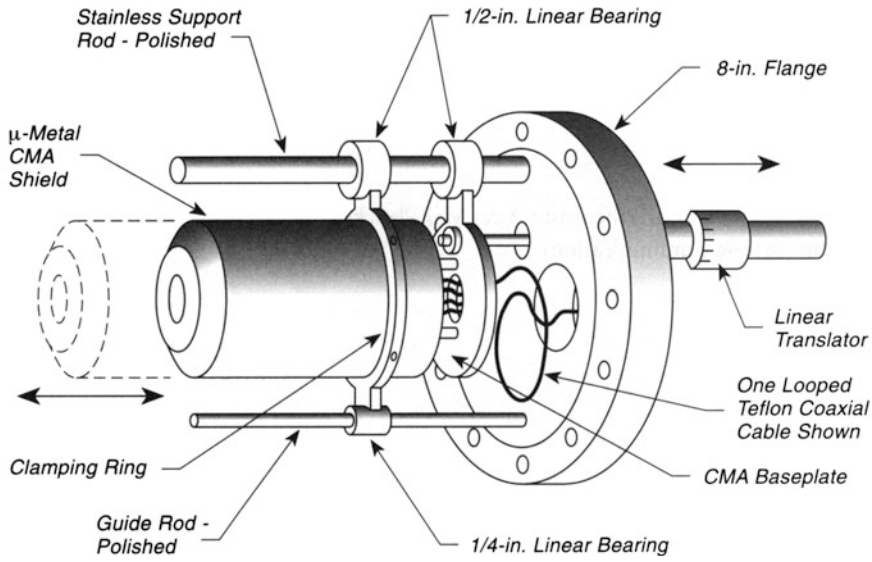

Fig. 1.11 Translating CMA auger spectrometer

Figure 1.11 shows a design [38] for translating a cylindrical mirror analyzer (CMA) Auger spectrometer over a 14-cm distance. This is done using a l/2-in.-diameter linear ball bearing [39] that slides on a polished stainless support rod at the top, and is guided along a 1/4-in.-diameter rod-linear bearing assembly on the bottom. The use of the smaller rod on the bottom allows the system to have a little flexibility to prevent seizure due to slight misalignment. The first upper support bushing is clamped with a stainless steel ring to the μ-metal shield of the CMA spectrometer using three set screws at 120° to each other. The second support bearing is attached to a baseplate that rigidly supports the CMA by rods. The entire assembly is mounted on an 8-in.-diameter Conflat flange. Translation is achieved using a small linear translator, mounted on a small flange, which pushes and pulls on the baseplate at a point close to the upper support rod to avoid torque on the upper bushing during motion.

The flexible electrical connecting wires are looped to give the needed extension and are made of Teflon-coated coaxial cable [40]. The coaxial cable is made UHV compatible by stripping off the outer cover, leaving the cable shield, and contributes no significant outgassing problem.

Another design for a translating Auger spectrometer may be found in [41]. In this case, the miniature instrument (electron optics 30 mm diameter; 45 mm length) is held on a single linear translator mounted on a 2 3/4-in.-diameter Conflat flange. The resolution of this instrument is $R = AE/E_o = 1.5\ \%$ [41].

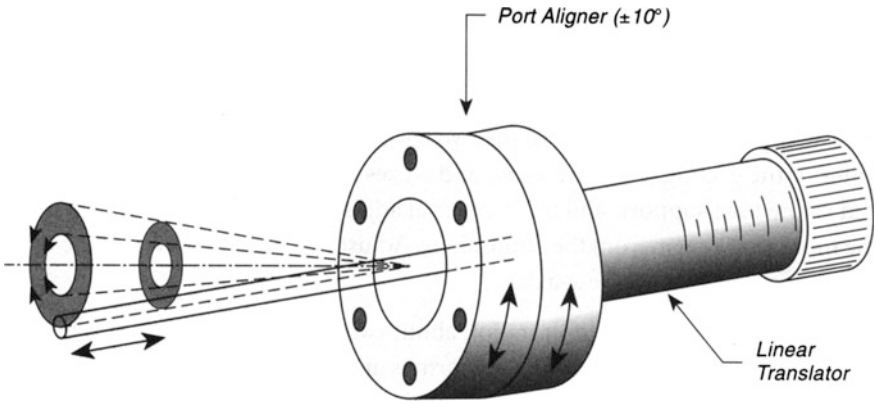

Fig. 1.12 Simple multiple motion

1.8 Simple Multiple Motion Manipulator

The provision of various degrees of motional freedom for samples, apertures, etc., in ultrahigh vacuum systems is often accomplished with complex manipulators such as that shown on p. 3. When complex motion is required and the measurement of the position of the sample is not required, more simple devices are possible. In Fig. 1.12, a device involving the combination of a port aligner and a linear translator is used to give multiple degrees of freedom for a rod. The port aligner allows ±10° motion within a solid cone, which is schematically shaded. The linear translator permits motion back and forth within this solid cone [42].

1.9 Simple Device for Small Rotations in Ultrahigh Vacuum—Grating Application

The rotation of gratings and other optical components through small angles in ultra high vacuum for the purpose of alignment is not straightforward. This device permits the adjustment of a grating through an angular range of less than 1° with ease [43]. Adjustments in one direction or in two are possible, depending on the structure used.

Figure 1.13a shows a side view of a device permitting one-dimensional rotation about the x-axis. Two planar broad-leaf springs are connected to a base support, and to a movable platform. A plane extrapolation of the two springs intercepts at the origin, *o,* which is the center of the grating. Here the *x*-, *y*-, and z-axes are defined. An adjustment rod is connected to the base support, and to an external adjustment screw. Bellows, as shown, isolate the mounting system from the atmosphere. Adjustment of the screw in the z-direction rotates the grating about the x-axis.

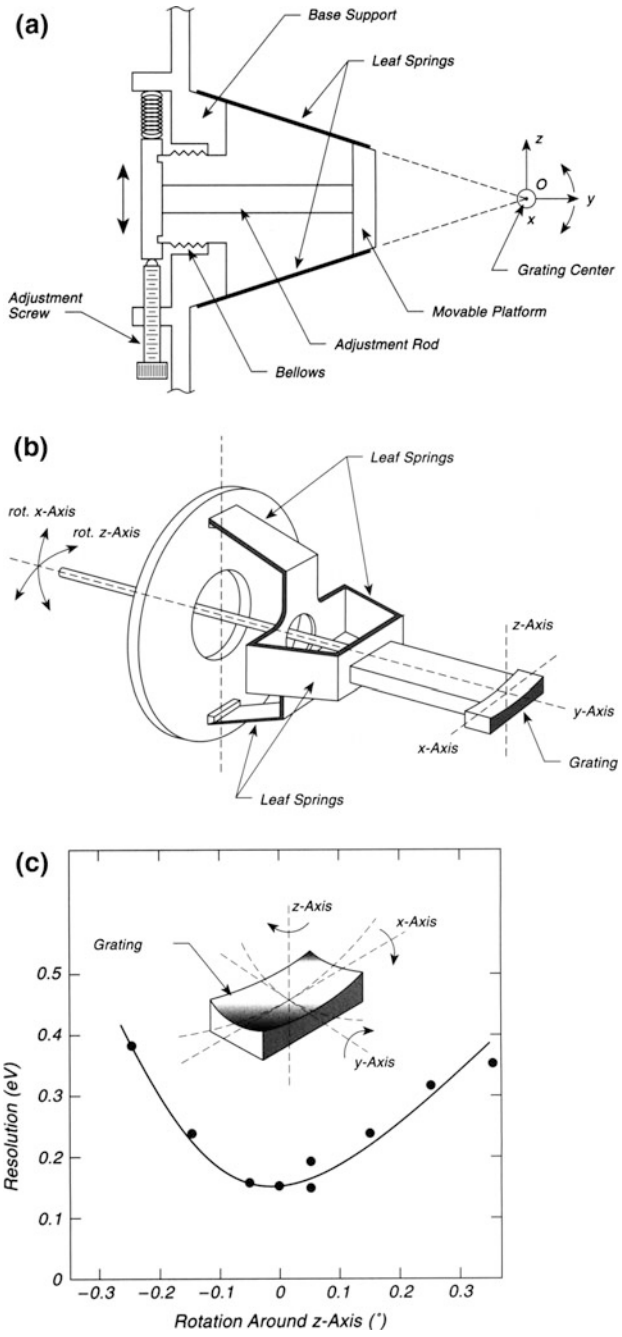

Fig. 1.13 Small rotations in UHV. **a** One-axis device. **b** Two-axis device. **c** Result—Z rotation

The principle can be extended to rotation about two axes, as shown in the schematic (Fig. 1.13b). Here, two sets of orthogonal leaf springs are used, and screws for rotation of the adjustment rod operate in the z- and x-directions, leading to grating rotation about the x- and z-axis.

Figure 1.13c shows the use of the two-axis device for optimization of the resolution of a UHV spectrometer. In this case, an angular resolution of less than 0.1° was achieved for optimum spectrometer resolution adjustment [43].

1.10 Turntable Rotation in Ultrahigh Vacuum

Figure 1.14 shows a turntable for the rotation of heavy equipment in UHV with high angular precision and repeatability, and without the need for coated or lubricated bearings. Rotation is achieved using a rotary feedthrough to move the axle of the turntable. The flat bottom of the turntable rests on three spheres made of a metal carbide mounted in a V-groove. The spheres are of 10-mm diameter and the three define the plane on which the turnable rotates. The mechanical stability is excellent, and several tens of kilograms may be supported. In addition, friction is low in ultrahigh vacuum. The danger of the spheres coming close to each other is small, especially when forward and backward motion is used alternatively. The system is uninfluenced by bakeouts at 200 °C [44].

1.11 Small Motions in UHV Systems Using Shape Memory Effect Alloys

An unusual phenomenon present in certain alloys may be used to make small motions in ultrahigh vacuum systems by the application of a small heating current to a helix of the alloy material. The shape memory effect (SME) is so named

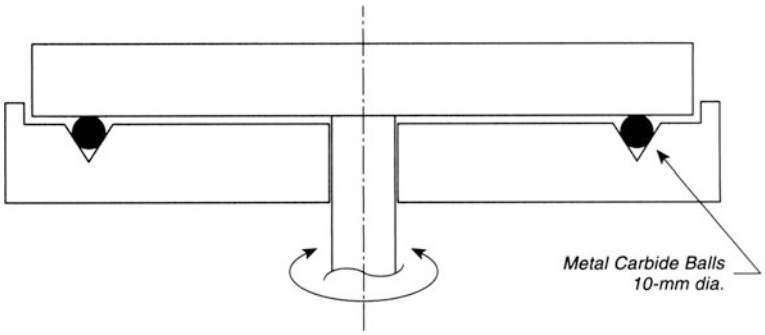

Fig. 1.14 Rotary platform

because shape memory alloy (SMA) wire helixes can be made to change from the "deformed" cold shape to the "preferred" hot shape reversibly. The restoring force. is quite large and may be used to achieve small motions as illustrated in the two examples shown here. There are numerous alloys that exhibit the SME, and a favorite SMA for UHV applications is NiTi. This material is easily formed into the hot shape and has a convenient transformation temperature. The shape change is caused by a transformation from a martensitic to an austenitic phase, with the high temperature austenitic material being produced at about 60 °C, while the reverse transformation occurs at about 30 °C. Deformations producing less that 2 % local strain in the martensitic state can be reversed by heating through the transformation temperature. By setting the hot shape in a helical wire it is possible to get extensions of several hundred percent without exceeding this strain limit.

Figure 1.15a shows a shutter arrangement made with a 0.45-mm-diameter NiTi wire [45]. The hot shape of the left-hand helix was set by winding it on a cylindrical mandrel and then heating to 500 °C for 1 h in a vacuum annealing oven to prevent oxidation. The helix was then stretched between two stainless steel posts and pinch clamped to each. The helix was therefore stretched from its preferred hot shape. Upon heating with a current of 2.5 A, the left segment of the helix contracts to its preferred hot shape, moving the attached shutter to the left in a period of less than 0.5 s. This operation stretches the right-hand cold helix beyond its plastic limit, which means that it has little restoring force. Thus, the heating current can be turned off after the shutter has moved to the left. To restore the shutter to its original position, one heats the right-hand portion of the helix.

The effect of bakeouts at 215 °C on a severely stretched (300 %) helix was tested over a 24-h period, and it was found that this treatment did not affect the hot shape memory [45].

A second example in which the SME is used to open and close a clamp on a manipulator is shown in Fig. 1.15b [46]. Here, the jaws of the clamp are opened when the NiTi SMA wire is heated. The particular wire [47] used here is of small diameter (0.15 mm) and has been treated in manufacture to exhibit a shorter length at high temperature and a longer length at low temperature. For strong clamping, four such wires were braided together and connected to a copper wire by a simple overhand knot above the ceramic insulator tube, which passes through the back end of the stationary upper jaw. The other end of the wire bundle is grounded through the jaw. A restoring force to close the jaws when the heating current is off is supplied by a spring mounted on a screw that is fixed in the upper jaw but that does not touch the lower jaw. When the lower jaw opens, this spring is compressed. Electrical heating to a wire temperature of 115 °C causes the jaws of the clamp to open up by about 2 mm when 0.21 A is passed through the four wires in vacuum. If the current is taken too high (0.23 A in vacuum), the annealing temperature will be exceeded, and the SMA wires will lose their pulling ability. The reader is referred to texts on the SME for more details [48, 49]. Also engineering studies of SME test structures are described in [50].

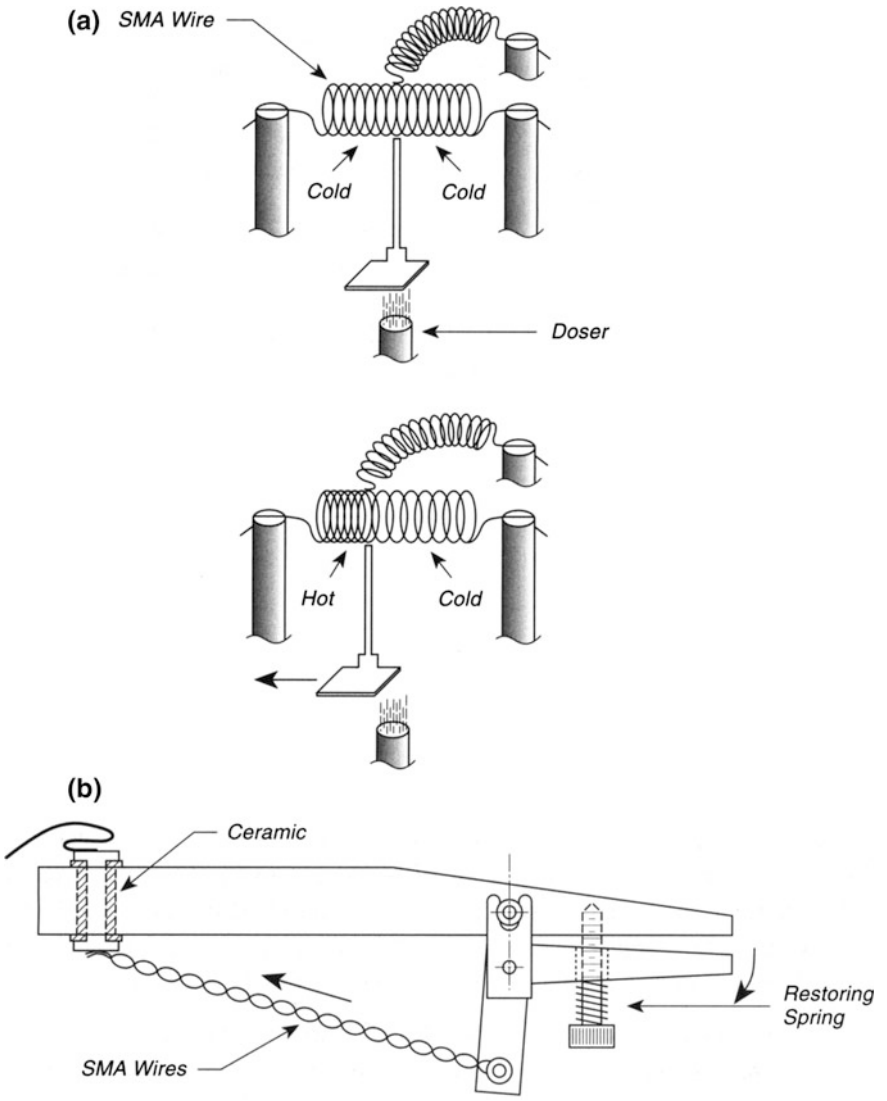

Fig. 1.15 Small motions using shape memory effect. **a** Shape Memory effect—Shutter. **b** shape memory effect—Clamp

1.12 Rotary Shutter Device Driven by Magnetic Eddy Current

The use of magnetic eddy currents in an ultrahigh vacuum system to drive a low friction shutter is illustrated in Fig. 1.16. The eddy current magnet, shown without its housing in the upper part of the Figure, drives the stepped copper rotor at

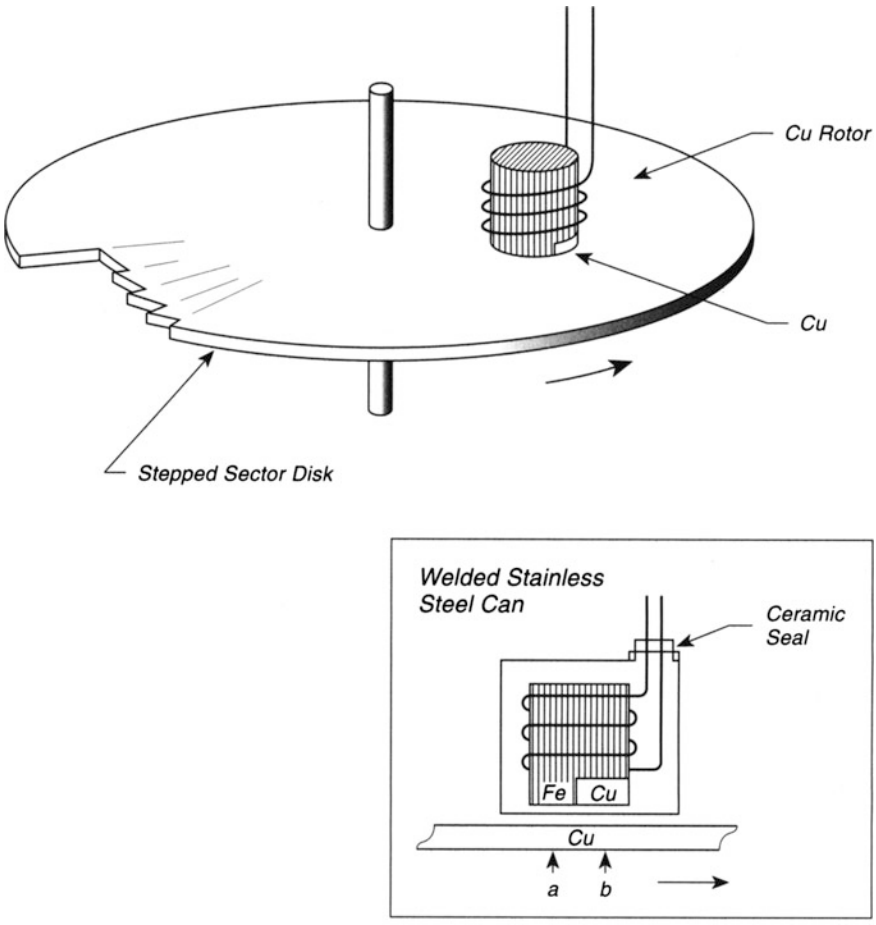

Fig. 1.16 Eddy current rotor

300 rpm when ball bearings are used, and 60-Hz power is applied to the coil. The copper disk is 0.8 mm in thickness. The stepped openings on the perimeter permit the operator to vary the open duty cycle for evaporations through the openings from an evaporation source mounted above the disk; operation near the perimeter gives larger fractional transmission than with the substrate placed more toward the axis.

The lower end of the iron cylinder (5 cm dia. × 7.5 cm long) contains a semi-circular piece of high-purity copper, 0.6 cm thick. It is wrapped with 150 turns of #14 (1.6 mm dia.) magnet wire with Formvar insulation. This is housed in a stainless steel can to prevent outgassing, and the can is welded shut using the ceramic feedthrough for electrical contact to the coil inside.

The device works on the basis of the lag of the magnetic field at position b from that at position a. This means that when the magnetic field is maximized during the

cycle at a, the eddy currents centered at b will also be maximized. A force on the volume element of the copper disk near *a* will be in the direction from *a* to *b*, and the disk will move. One quarter cycle later, the magnetic field at *b* will interact with the eddy currents centered at *a* and the force is again in the direction from *a* to *b*. During the next half cycle, both the magnetic field and eddy current directions are reversed, again giving a force in the same direction. A mechanical brake is employed to stop the rotation.

The shutter device is used to reduce the flux of evaporating material arriving at the substrate by a precise geometrical method involving only the dimensions of the transmission slots relative to the circumference of the sector disk. Thus, thick films deposited near the outer edge of the disk are proportionately reduced to thinner films deposited at a known radius under the disk. Measurements of the film thickness deposited above the shutter can be converted to sector thicknesses below the shutter [51]. A similar device, driven conventionally, for extending the range of a quartz microbalance has been described previously [52].

1.13 High-Speed Ultrahigh Vacuum Motor

A modified hysteresis-synchronous motor was designed to eliminate most of the outgassing that occurs during motor operation [53]. There are two sources of gas evolution in motors working in vacuum. The first is outgassing of the bearings. The second is outgassing of the stator winding insulation owing to heating during operation.

The design shown in Fig. 1.17 eliminates both of these effects to a high degree. The bearings [54] in the motor [55] were lubricated with a dry lubricant. The stator was isolated from the vacuum system and the rotor by a container sealed with two O-ring seals at either end. This container is filled with nitrogen to 1 atm to facilitate heat conduction away from the motor. Cooling coils that are brazed to the outside of the isolation container maintain low temperatures at the motor.

The main modification in the motor involved increasing the gap between rotor and stator to allow the isolation container wall (0.010 in. thick) to fit. This may be done in two ways. Either the inside diameter of the stator is increased, in which case the isolation container wall must be of magnetic stainless steel (this was done), or if the outer diameter of the rotor is decreased, the isolation container wall between rotor and stator must by made of nonmagnetic stainless steel.

Motors modified in this way have been working for more than one year at 200 Hz and exhibit a pressure rise of less than 1×10^{-9} Torr [53].

To reduce the loss of gas still further, the motor housing could be filled with nitrogen gas at about 1 Torr pressure, which is still adequate for heat transfer. Alternatively, UHV sealants might be used to seal the motor [56].

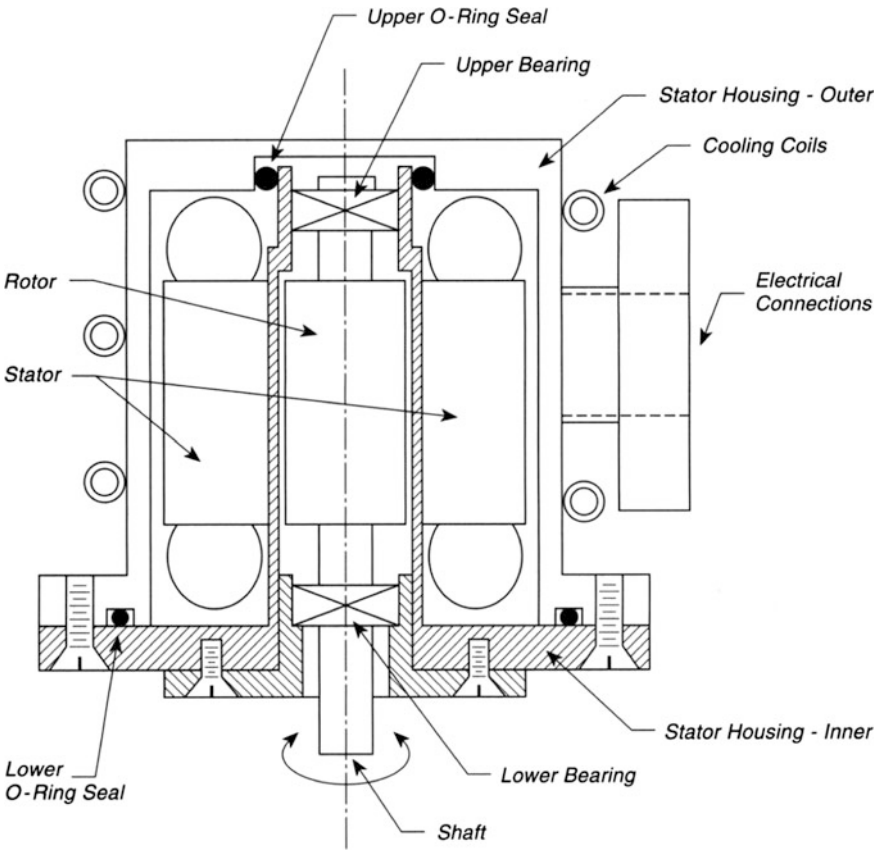

Fig. 1.17 High-speed UHV Motor

1.14 High-Speed Rotary Feedthrough for UHV Operation

A simple rotary feedthrough, suitable for high-speed rotation in an ultrahigh vacuum system, is shown in Fig. 1.18. The device uses a hysteresis motor, in which the stator is externally mounted, for driving a shaft at speeds from 1200 to 15,000 rpm [57]. The pressure rise during operation is less than 1×10^{-10} Torr, since the stator, which generates gas on heating, is isolated from the vacuum system.

In the Figure, a shaft, held between two unlubricated bearings [58], is attached to a rotor and both pieces are ground together to assure good dynamic balance. Two spring washers eliminate axial play. The stator is held in place by plastic supports. The torque delivered is limited by the motor size chosen [59] and by the gap between stator and rotor, which is 1.5 mm here. After 1200 h of intermittent operation, no need for bearing replacement was encountered.

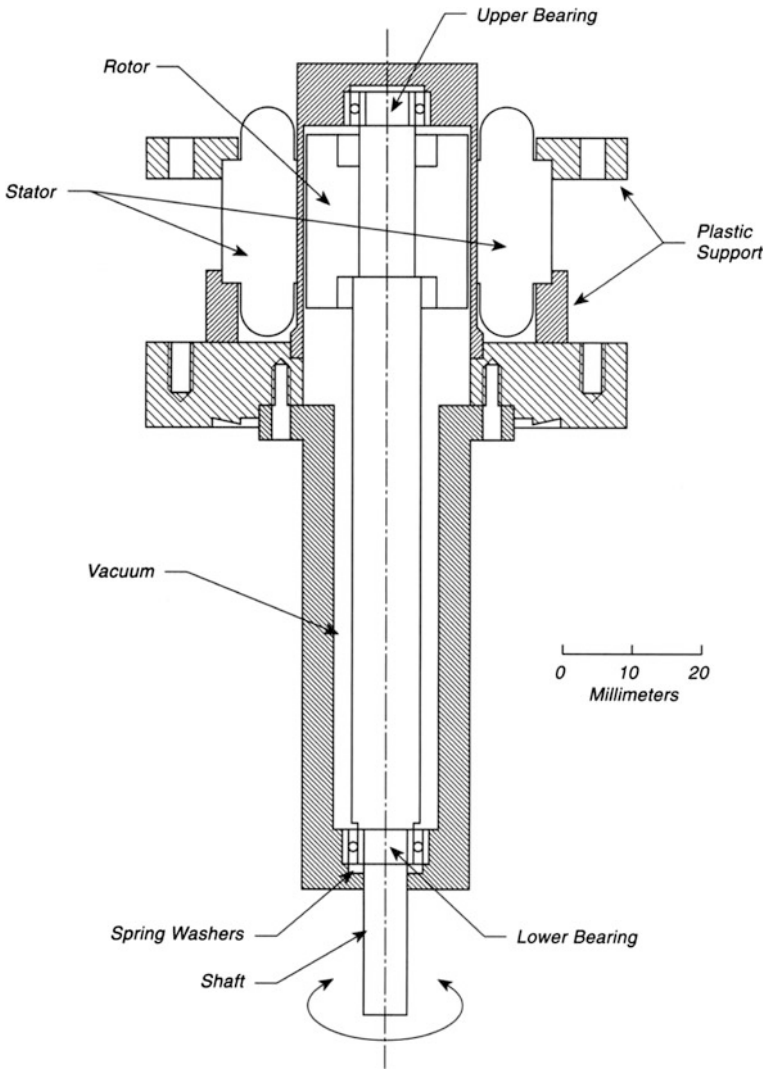

Fig. 1.18 Very high speed UHV motor

1.15 Self-lubricating Bearings in UHV

The use of boron nitride, BN, as a bearing lubricant has been demonstrated for light loads in a combination rotary-translator bearing [60]. This is especially convenient for magnetically driven shafts where only small forces may be applied.

Figure 1.19 shows an exploded view of the bearing assembly. The rotary and translation shaft, made of stainless steel, is supported at some distance from the

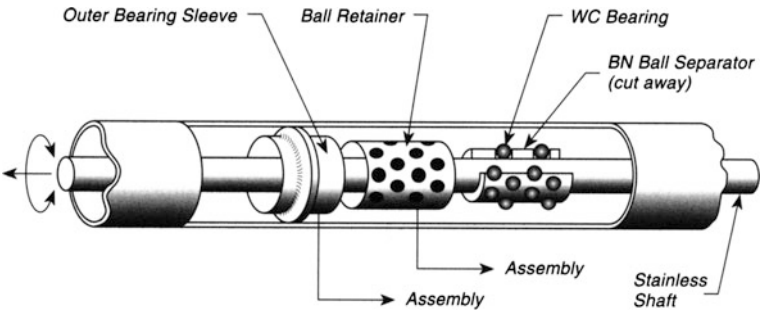

Fig. 1.19 Exploded view—self-lubricating translation-rotation bearing

bearing by V-blocks that can be moved into contact with the shaft, and these are not shown here. The shaft is held by WC bearings (0.48 cm diameter) which themselves are held in a BN ball separator cylinder containing holes that accommodate the WC balls. This BN ball separator provides continuous lubrication to the WC balls and the rod, since BN is a dry lubricant. The balls are held in their place by a type 6061 Al alloy retainer which slips over the top of the balls keeping them from touching each other. An outer-bearing sleeve then slips over all of the components and is stabilized by contact with the inside of the vacuum wall tubulation. The bearing assembly is loosely retained between the magnetic drive mechanism and a stop on its other end, not shown.

The system can be repeatedly baked at 275 °C. Since BN is hygroscopic, when the chamber is open to atmosphere, the bearing is kept at 80–100 °C using heating tape on the outside of the tubulation. No contamination of samples by BN has been detected using various surface analysis methods.

1.16 Lubrication for Heavy Sliding Loads in Ultrahigh Vacuum

The lubrication of metal/metal interfaces for sliding motion in ultrahigh vacuum is a special problem related to the fact that practical surfaces that often slide together with low friction in air will seize in vacuum because of the absence of adsorbed molecular layers of water lubricant or other materials.

Figure 1.20a shows a test device used to evaluate the lifetime of a special coating on stainless steel surfaces that was able to lubricate bearing surfaces successfully for over 200,000 cycles. The comparable unlubricated surfaces failed after 1740 cycles [61].

A ballscrew that translates over spherical bearings in a race was installed, along with a parallel identical partner ballscrew behind the device plane (not shown), in a device which drove a 2-kg mass up and down in ultrahigh vacuum of the order of

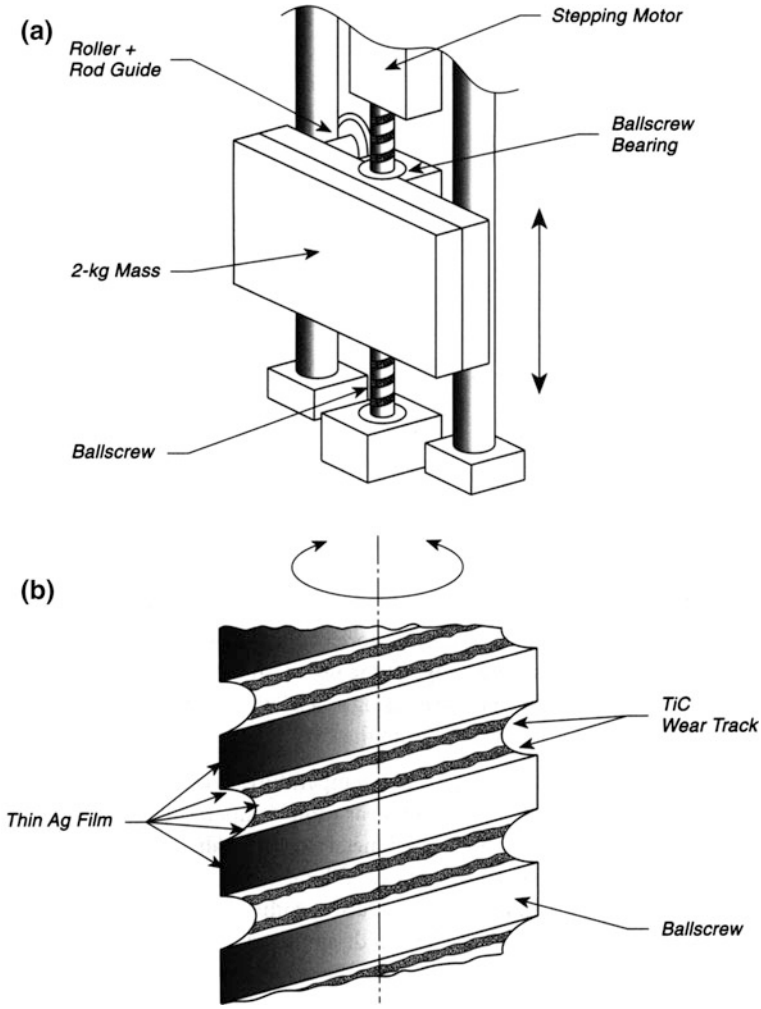

Fig. 1.20 Heavy load lubrication in UHV. **a** Ballscrew test device. **b** Wear track patterns

10^{-10} Torr. The vacuum condition was achieved after a bakeout at 140 °C. The motion drove the mass upward and downward 45 mm, at a speed of 2.25 mm/s. The screws and nuts of the ballscrews are made of 440C stainless steel, finished using electrochemical buffing to a roughness of about 0.1 μm, and then coated as described below.

The ballscrew was coated with a TiC film, 1.5 μm in thickness, and with a micro-Vickers hardness of about Hv 1100. An Ag coating of 0.3-μm thickness was then applied. The ball bearings mating to the ballscrew were also made of 440C stainless steel, coated with an Ag film of 0.3-μm thickness. The unlubricated surface, used as a control, was not treated with either TiC or Ag.

Figure 1.20b shows the wear track observed visually after 200,000 cycles. The thin-film Ag coating is still retained on sections of the screw that did not undergo contact with the balls. The TiC underlayer is visible in the contact regions and was not worn through. Surprisingly, when the device was operated in air, the untreated ballscrew performed well but the coated ballscrew did not move smoothly.

Plasma-coated Ag films on stainless steel screws for use in UHV have been found to resist cold welding [62]. Also, ordinary Ag plating of either the bolt threads or the nut threads of stainless steel bolts used internally or externally in baked UHV systems is reported to be an excellent lubricant using coatings of 10-μm thickness [63]. It has been found that coating metals such as Ta, Cu, Mo, and stainless steel with an oxide film, by heating to redness in air, will provide protection against galling during motion in UHV [64].

A good review on tribology and lubrication in the vacuum environment in space is found in [65].

1.17 Simple UHV Bearing for High-Speed Shafts

Steel ball bearings are often used unlubricated in ultrahigh vacuum. At high rotational speeds, over time, these bearings tend to become sticky before final seizure. The development shown in Fig. 1.21 uses polytetrafluoroethylene (PTFE or Teflon) as a bearing material for continuous rotation at 10–1000 rpm. The bearing is machined using sharp oil-free tools, and care is taken not to introduce metallic particles into the PTFE. Cleaning is carried out in organic solvents, and traces of metal and oil may be removed by use of hot nitric acid solution, followed by soaking in distilled water.

The design has three essential components. The first is the use of relief slots made by a small, round file at 90° intervals around the inside of the bearing. Removal of about one-third of the contact area was found to be essential. The second feature is the placing of pumping holes in the PTFE bearing, and more of these can be supplied on the upper housing. The third feature of the design is the use of an 0.25–0.50-mm-diameter wire squeezed between the bearing and the housing as a friction point to prevent the bearing from rotating when torque is supplied from the shaft.

Bakeout below 200 °C is appropriate, and temperatures above about 250 °C are to be avoided. The bearing should be operated near room temperature and the mechanical admission to the bearing surface of flakes of metal from thin film deposition in the chamber should be avoided. Small partial pressures of fluorine and chlorine were seen initially, and these decreased with time. Initial use also produced small partial pressures of methane and carbon monoxide which soon disappeared. The rotary bearing was used with a 400 rpm shaft for a million rotations without any apparent degradation [66].

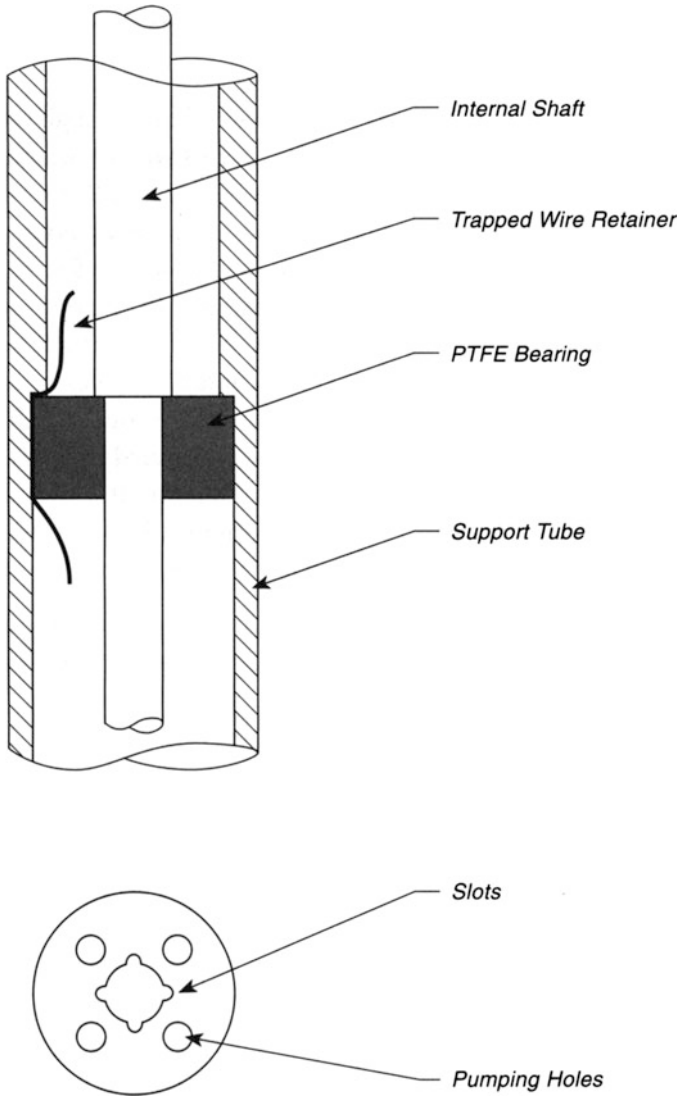

Fig. 1.21 Internal rotary bearing

1.18 Flange-Mounted UHV Variable Aperture

The need for an internal aperture that can be adjusted in ultrahigh vacuum exists both in optical experiments and also in vacuum systems where variable pumping speed control is desired. An inexpensive aperture device is shown in Fig. 1.22. It consists of a variable iris aperture [67] that may be purchased as a component, mounted inside a 2 3/4-in.-diameter Conflat flange. The aperture is mounted on an

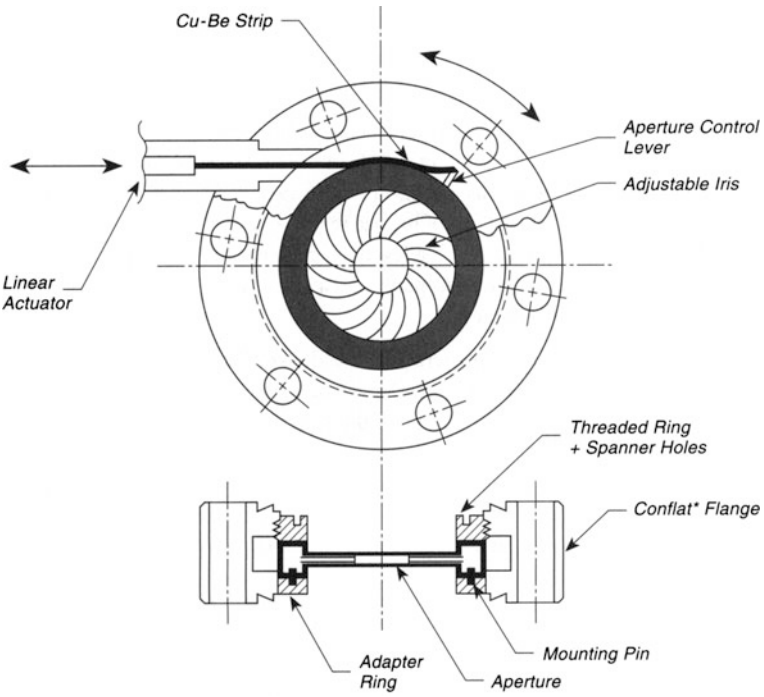

Fig. 1.22 Adjustable UHV Aperture

adapter ring that is tack welded into the flange to avoid distortion. The aperture is fixed from rotation by mounting pins that fit into the adapter ring and through the wall of the aperture housing. The aperture is tightened into place by a threaded ring containing holes for a spanner wrench. The original Conflat flange has had an inside slot milled around its inner circumference for the motion of the aperture control. This is accomplished by a linear actuator coupled to the aperture control lever by a Cu-Be strip (0.3 mm thick) that extends around the aperture housing inside the milled slot. The aperture is degreased before use and relubricated with a tiny amount of MoS_2 applied lightly with a cloth.

The iris opening ranges from 1 to 25 mm and can be reproduced to a precision of 2 % if one is careful to avoid backlash by moving always in the same direction for final adjustment [68].

1.19 Linear Motion Platform (LMP)

A clever mechanical design to convert a linear screw motion into a linear platform motion with reduced amplitude has been described by Dr. H.P. Rust and Mr. L. Cramer [69]. The design is used as an approach mechanism for an STM tip in a low-temperature instrument [70].

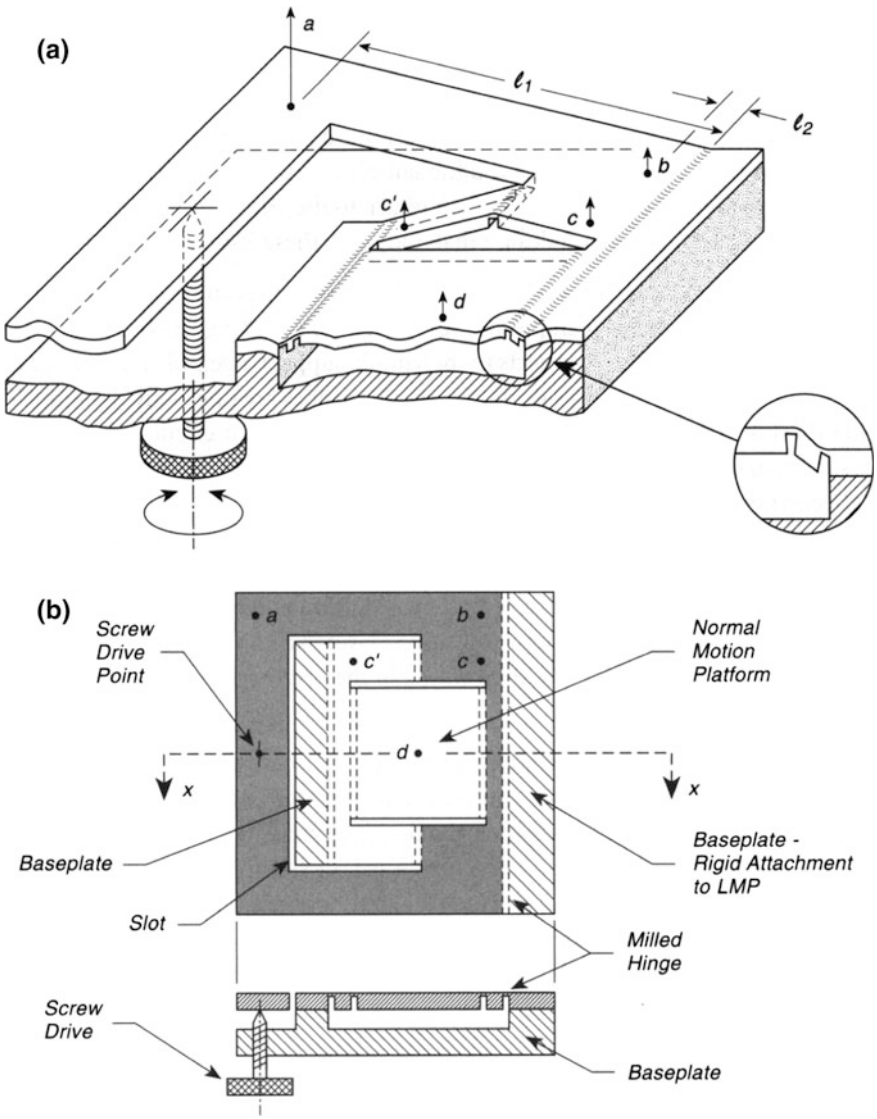

Fig. 1.23 Linear movable platform. **a** 3D-sectional view of portion of LMP. **b** Top and sectional view (x–x)

The device shown in Fig. 1.23a, b is made entirely from a single piece of bronze, which, after fabrication, is rigidly attached to a base plate also made of bronze. The active LMP part is milled with three orthogonal slots in the form of a C, and then 6 "milled hinge" cavities are also produced as shown in Fig. 1.23b by dashed lines. These milled hinge cavities have only a thin section of bronze remaining at the top

of each cavity, giving excellent bending response through a few degrees. The LMP is then rigidly attached to the two projecting flats from the baseplate, and a screw motion, schematically shown as a thumbscrew, is added on the left.

The device works as follows. As the screw is moved up or down, the plate section above it moves up or down, and we will assign a length of motion a as shown in Fig. 1.23a. This motion is reduced at point *b* by virtue of the relative length of the arms involved as the milled hinge is bent near the point *b*. The section of the LMP device labeled *c* is rigidly connected to the outer plate section containing the *a* and *b* motions, and there is therefore an equivalent *c* motion as shown, i.e., $b = c$. As section *c* moves up, a milled hinge, midway between *c* and *c'* flexes as a result of the forces it experiences. This causes a symmetrical distortion in the bridged section *c*–*c'* and leads to equal angular displacement on both ends of the platform, which occurs as a result of distortions in the region of the pair of milled hinges on each end of the platform. The small motion of the platform is schematically indicated by *d*. Because of the symmetry, the motion of the platform up and down will be in the normal direction without any tilting, which is the desired result.

The function of the device can best be understood by remembering that the light gray region, shown in Fig. 1.23b, and containing *a*, *b*, and *c* and the symmetrically similar regions, is rigid and undergoes identical angular distortion away from the baseplate when the screw is advanced. The mechanical advantage is given by the ratio of the lever arms, l_1 and l_2.

1.20 Vacuum Trolley Transport System

The transport of samples from one vacuum system to another, where different preparation and measurement methods are used, is a common necessity in UHV measurements, as only so many techniques may be used in a single vacuum chamber. A trolley system can be used to make this transport, and the system shown has the capacity to transport 4 samples at one time, dropping them off amongst 5 vacuum systems. Magnetic transfer is used to insert a sample holder into the trolley system from the loading chamber at the third position from the left. A screw advance mechanism moves the samples laterally in 4 special sample holders which are designed as locking devices. The locking sample holders, shown schematically on the trolley in the insert to Fig. 1.24, are used to hold the samples. Engagement of each sample holder by the magnetic transfer device allows the sample holder to be inserted and locked by rotation on centrally-located sample stages in each system. While this device has maximum versatility for simple analysis at various locations, heating of the samples inside the vacuum chambers will require reversible electrical connections for both electrical heating power and thermocouples as described elsewhere in this book [71].

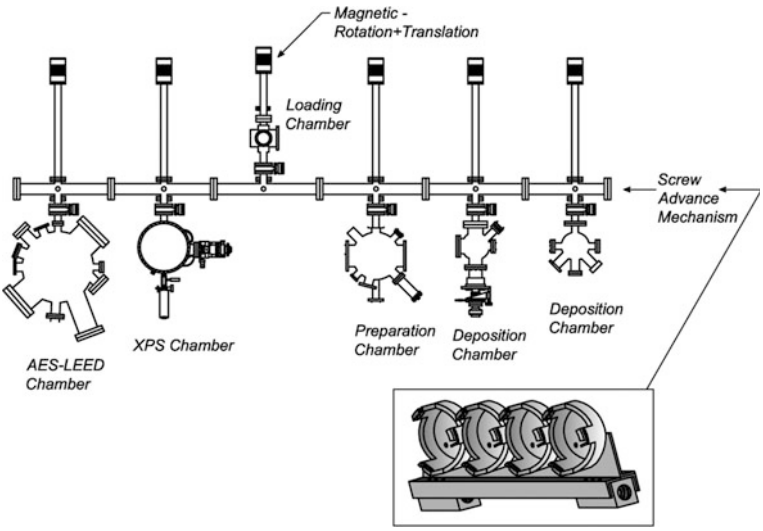

Fig. 1.24 Vacuum trolley transport system—4 samples

1.21 Thermally Compensated STM with Repeatable Sample Positioning

Two problems common to most STM designs have to do with the thermal drift of the relative position of the STM tip and the sample and the inability to replace a sample in the same position so that the STM tip can return to the same image point. Both of these problems have been solved by a design that addresses these issues [72].

Figure 1.25a shows a side view of the STM design. Two piezotubes are mounted on the same base. The inner tube (scan piezotube) is used for scanning the tip, while the outer tube (translation piezotube) connects to the sample support assembly and is used to support and translate this assembly. Both of these piezotubes are of exactly the same length, so that thermal drifts are compensated in the z-direction; their circular symmetry eliminates thermal drifts in the x, y-directions. The outer translation piezotube is surrounded by a thermal shield, made of oxygen-free high conductivity (OFHC) Cu to eliminate temperature gradients, which would defeat the principle of having two identical-length piezotubes for compensation of thermal drift effects. The outer tube is connected to the sample holder through a quartz mounting assembly that consists of an outer quartz tube and a quartz or metal/ceramic sample holder. The sample holder slides (by means of five spherical bearing contacts) on two metallized quartz rails that are mounted inside the outer quartz tube as shown in Fig. 1.25b. Operation of the translator piezodrive causes the sample to jump toward the tip as a result of the friction and inertia effects in the sample holder, and adjustment of the piezo activation waveform can be used to

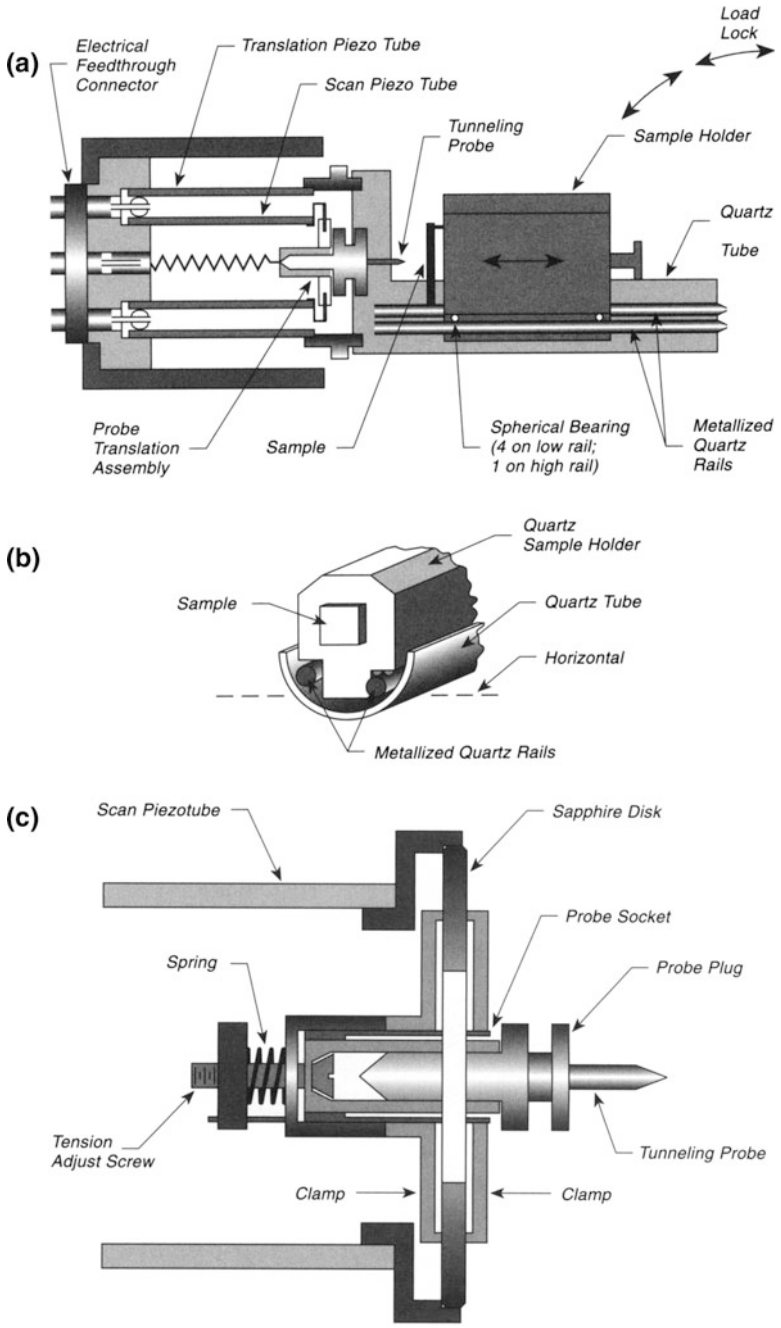

Fig. 1.25 Thermally compensated STM—repeatable sample positioning. **a** Side view. **b** Sample holder. **c** Detail, probe translator

produce jumps from about 10^4 Å to less than 5 Å. By working in the kHz frequency domain, translation rates up to 1 mm/s are possible.

The sample holder may be removed from the outer quartz tube containing the rods and the sample may be transferred and heated in a furnace or in a load lock. Upon return of the sample holder to the quartz rods, the design permits repositioning to an accuracy of several thousand Å, depending upon how much the sample is bumped during transfer. This is accomplished by using gravity to align the sample on the rails, which are tilted with respect to the horizontal plane. The repositioning scheme, using gravity to set the sample on the rails in the same position, is based on kinematic design principles that are well described elsewhere [73].

The details of the construction of the probe translator are shown in Fig. 1.25c.

The thermal drift experienced by this design is about 1 Å/h.

A piezo-driven translator for the tip, which moves in the *x*, *y*-directions over several millimeters by a stepping and gripping action, thereby eliminating mechanical positioning devices, has been described as a modification of this device [74].

References

1. P. Toennies, Max Planck Institut Stroemungsf, Bunsenstr. 20, D-37073 Göttingen, Germany (private communication)
2. D. Venus, Rev. Sci. Instrum. **62**, 1361 (1991)
3. Y. Dai, H. Li, F. Jona, Rev. Sci. Instrum. **61**, 1724 (1990)
4. T. Engel, D. Braid, E.H. Conrad, Rev. Sci. Instrum. **57**, 487 (1986)
5. J.J. Zinck, W.H. Weinberg, Rev. Sci. Instrum. **56**, 1285 (1985)
6. K.D. Jamison, F.B. Dunning, Rev. Sci. Instrum. **55**, 1509 (1984)
7. N.J. Wu, A. Ignatiev, Rev. Sci. Instrum. **56**, 752 (1985)
8. J.A. Stroscio, W. Ho, Rev. Sci. Instrum. **55**, 1672 (1984)
9. J. Larscheid, J. Kirschner, Rev. Sci. Instrum. **49**, 1486 (1978)
10. K.D. Jamison, F.B. Dunning, Rev. Sci. Instrum. **55**, 1509 (1984)
11. H. Durr, Th Fauster, R. Schneider, J. Vac. Sci. Technol. **A8**, 145 (1990)
12. M. Michaud, P. Cloutier, L. Sanche, Rev. Sci. Instrum. **66**, 2661 (1995)
13. R.R. Wilson, Rev. Sci. Inst. **12**, 91 (1941)
14. V.R. Unwin, K. Horn, P. Geng, Vakuum Tek **29**, 149 (1980)
15. M.F. Zabielski, R.R. Blaszuk, J. Vac. Sci. Tech. **13**, 644 (1976)
16. J.T. Yates, Jr. (unpublished)
17. J.J. Zinck, W.H. Weinberg, Rev. Sci. Inst. **56**, 1285 (1985)
18. A. Pararas, S.T. Ceyer, J.T. Yates Jr, J. Vac. Sci. Tech. **21**, 1031 (1982)
19. E. Puckrin, J.K. Fowler, A.J. Slavin, J. Vac. Sci. Tech. **A7**, 2818 (1989)
20. D.J. Auerbach, C.A. Becker, J.P. Cowin, L. Wharton, Rev. Sci. Inst. **49**, 1518 (1978)
21. The spring-loaded Teflon seals are available in many sizes from the Fluorocarbon Corporation, 10871 Kyle Street, P.O. Box 520, Los Alamitos, CA 90720. Their descriptive literature gives many details about the seals and the preparation of the metal surfaces on which they ride
22. S.M. George, J. Vac. Sci. Tech. **A4**, 2394 (1986)
23. J.A. Stroscio, W. Ho, Rev. Sci. Inst. **55**, 1672 (1984)
24. P.A. Thiel, J.W. Anderegg, Rev. Sci. Instrum. **55**, 1669 (1984) (A particularly nice design of a manipulator with an easily demountable cold finger end for crystal replacement can be found)

25. R.A. Kubiak, P. Stonestreet, S.M. Newstead, E.H.C. Parker, T. Whall, N. Naylor, J. Vac. Sci. Technol. **A9**, 2797 (1991)
26. J. Larscheid, J. Kirschner, Rev. Sci. Instrum. **49**, 1486 (1978)
27. K.D. Jamison, F.B. Dunning, Rev. Sci. Instrum. **55**, 1509 (1984)
28. H. Durr, Th Fauster, R. Schneider, J. Vac. Sci. Technol. **A8**, 145 (1990)
29. P. Feulner, D. Menzel, J. Vac. Sci. Technol. **17**, 662 (1980)
30. H. Schlichting, D. Menzel, Surface Sci. **285**, 209 (1993)
31. H. Schlichting (private communication)
32. Obtainable from Acheson Colloids, 1607 Washington Avenue, P.O. Drawer 611747, Port Huron, MI 48061-1747
33. T. Gog, S.M. Durbin, Rev. Sci. Instrum. **60**, 3030 (1989)
34. R.W. Bertram, J. Vac. Sci. Tech. **7**, 612 (1970)
35. C.M. Rouleau, R.M. Park, J. Vac. Sci. Tech. **A11**, 464 (1993)
36. MSC, 151 Sunnyside Boulevard, Plainview, Long Island, New York, 11803
37. H. Gutleben, J.T. Yates Jr, J. Vac. Sci. Tech. **A9**, 170 (1991)
38. M.C. Reuter, R.M. Tromp, J. Vac. Sci. Technol. **A6**, 2575 (1988)
39. 1/2 in. -Thompson A-81420-SS; 1/4 in.—Thompson A-4812-SS
40. Custom Cable Corp., 242 Butler Street, P.O. 1050, Westbury, NY 11590-3193. Cable type: RG 316/V
41. D.N. Mcllroy, P.A. Dowben, A. Knop, E. Rühl, J. Vac. Sci. Technol. **B13**, 2142 (1995)
42. Dr. Oliver Schaff, Fritz Haber Institut der Max Planck Gessellschaft, Faraday Weg 4-6, D-14195 Berlin (private communication)
43. W.A.M. van Bers, A.J.J. Franken, P.K. Larsen, Rev. Sci. Instrum. **54**, 637 (1983)
44. W. Stocker, K.H. Rieder, J. Vac. Sci. Tech. **A2**, 1606 (1984)
45. A.P. Jardine, M. Ahmad, R.J. McClelland, J.M. Blakely, J. Vac. Sci. Tech. **A6**, 3017 (1988); This idea is based on an earlier paper which also characterizes the behavior of a similar device as a function of repeated cycling; see B.J. Mulder, Vacuum **26**, 31 (1976)
46. W.F. Smith, E.E. Ehrichs, A.L. de Lozanne, J. Vac. Sci. Tech. **A10**, 576 (1992) (This article contains additional references to other devices constructed with SME alloys)
47. The thicker SME wire used in Figure 11A was obtained from RayChem, 300 Constitution Drive, Menlo Park, CA 94025
48. J. Perkins (ed.) *Shape Memory Effects in Alloys* (Plenum, New York, 1975)
49. T.W. Duerig, K.N. Melton, Proc. Mater. Res. Soc, Int. Meet. Adv. Mater. **9**, 581 (1989)
50. M. Nishikawa, M. Kawai, T. Yokoyama, T. Hoshiya, M. Naganuma, M. Kondo, K. Yoshikawa, K. Watanabe, J. Nucl. Matls. **179–181**, 1115 (1991)
51. J.S. Brooks, R. Meservey, R.K. MacNabb, J. Vac. Sci. Tech. **20**, 243 (1982)
52. F.C. Wilson, D.B. Sandstrom, H.B. Serreze, Rev. Sci. Instrum. **46**, 1593 (1975)
53. T. Engel, D. Braid, Rev. Sci. Instrum. **56**, 1668 (1985)
54. Barden Bartemp bearings, SR 188 SSTB
55. Globe motor, model 75 A 1003-2
56. Professor Thomas Engel, Department of Chemistry, BG-10 University of Washington, Seattle, WA 98195 (private communication)
57. T. Engel, Rev. Sci. Instrum. **52**, 301 (1981)
58. The bearings were from Barden Bartemp, Type SR 188 SSTB
59. The rotor and stator were obtained from KaVo Electrotechnisches Werk GmbH D-7970 Leutkirch, Germany, Type EV 48-15
60. G.J. Collet, E.L. Garwin, R.E. Kirby, Rev. Sci. Instrum. **58**, 479 (1987)
61. H. Saeki, J. Ikeda, I. Kohzu, H. Ishimaru, J. Vac. Sci. Technol. **A8**, 3360 (1990)
62. R.A. MacGill, R.A. Castro, X.Y. Yao, I.G. Brown, J. Vac. Sci. Technol. **A12**, 601 (1994)
63. A. Contaldo, Rev. Sci. Instrum. **36**, 1510 (1965)
64. W.F. Egelhoff, National Institute of Standards and Technology, Gaithersburg, MD 20899-0001 (private communication)
65. E.W. Roberts, M.J. Todd, Wear **136**, 157 (1990)
66. R.A.A. Kubiak, P. Driscoll, V. Manning, R. Houghton, J. Vac. Sci. Tech. **A4**, 1951 (1986)

67. Edmund Scientific Company, 101 East Gloucester Pike, Barrington, NJ 08007-1380
68. F. Homan, J. Vac. Sci. Tech. **17**, 664 (1980)
69. Registered design: H.-P. Rust, L. Cramer, Deutsches Patentamt Gebrauchsmuster No. G94 12 112.5, (27 July 1994)
70. H.-P. Rust, J. Buisset, E.K. Schweizer, L. Cramer, Rev. Sci. Instrum. **68**(1), Jan 1997
71. J. Szuber, private communication
72. J.W. Lyding, S. Skala, J.S. Hubacek, R. Brockenbrough, G. Gammie, Rev. Sci. Instrum. **59**, 1897 (1988); also, U.S. Patent 4,841,148
73. E.B. Wilson, *An Introduction to Scientific Research*, 1st edn. (McGraw Hill, NY, 1952)
74. R.T. Brockenbrough, J.W. Lyding, Rev. Sci. Instrum. **64**, 2225 (1993)

http://www.springer.com/978-3-319-17667-3

Experimental Innovations in Surface Science
A Guide to Practical Laboratory Methods and Instruments

Yates Jr., J.T.

2015, XXI, 655 p. 322 illus., Hardcover
ISBN: 978-3-319-17667-3